A revision of the Combined Drought Indicator (CDI) used in the European Drought Observatory (EDO)

Carmelo Cammalleri[1,*], Carolina Arias-Muñoz[2], Paulo Barbosa[1], Alfred de Jager[1], Diego Magni[3], Dario Masante[3], Marco Mazzeschi[4], Niall McCormick[1], Gustavo Naumann[1], Jonathan Spinoni[1] and Jürgen Vogt[1]

[1] European Commission, Joint Research Centre (JRC), Ispra, Italy.

[2] Arhs Developments, Milan, Italy.

[3] Arcadia SIT, Vigevano, Italy.

[4] UniSystems Luxembourg Sàrl, Luxembourg.

[*] C. Cammalleri (carmelo.cammalleri@ec.europa.eu)

Abstract

Building on almost ten years of expertise and operational application of the Combined Drought Indicator (CDI), which is implemented within the European Commission's European Drought Observatory (EDO) for the purposes of early warning and monitoring of agricultural droughts in Europe, this paper proposes a revised version of the index. The CDI conceptualizes drought as a cascade process, where a precipitation shortage (WATCH stage) develops into a soil water deficit (WARNING stage), which in turn leads to stress for vegetation (ALERT stage). The main goal of the revised CDI proposed here is to improve the indicator's performance for those events that are currently not reliably represented, without altering either the modelling conceptual framework or the required input datasets. This is achieved by means of two main modifications: (a) use of the

previously occurring CDI value to improve the temporal consistency of the time series, (b) introduction of two temporary classes - namely TEMPORARY RECOVERY for soil moisture and vegetation greenness, respectively - to avoid brief discontinuities in a stage. The efficacy of the modifications is tested by comparing the performances of the revised and currently implemented versions of the indicator for actual drought events in Europe during the last 20 years. The revised CDI reliably reproduces the evolution of major droughts, out-performing the current version of the indicator, especially for long-lasting events, and reducing the overall temporal inconsistencies in stage sequencing of about 70%. Since the revised CDI does not need supplementary input datasets, it is suitable for operational implementation within the EDO drought monitoring system.

Keywords: agricultural drought, SPI, soil moisture, FAPAR, drought monitoring.

1. Introduction

In the past 20 years, the monitoring of drought events has gained increasing relevance thanks to the shift in the paradigm for drought risk management from a reactive to a proactive approach (Wilhite and Pulwarty, 2005). As advocated by WMO and GWP (2014), drought monitoring and early warning systems represent one of the three main pillars for successful integrated drought management (the others being vulnerability and impact assessment, and drought preparedness, mitigation, and response). A drought monitoring and early warning system identifies climate and water resources trends and detects the emergence or probability of occurrence and the likely severity of droughts and its impacts, and should provide reliable information about impending drought conditions that can be timely communicated to water managers, policy makers, and the public (Vogt et al., 2018a).

As highlighted in WMO and GWP (2016), monitoring the different aspects of drought may

require a variety of drought indicators and indices. In particular, the authors distinguish among three typologies of index-based monitoring systems: i) single indicator, ii) multiple indicators, and iii) composite or hybrid indicators. The latter group allows the integration of a potential large number of elements into the assessment process of drought characteristics.

A progenitor in the composite indicator category is the approach developed in the United State Drought Monitor (https://droughtmonitor.unl.edu), based on an expert-supervised combination of a percentile ranking of several indices for a weekly-based index (Svoboda et al., 2002). Another combined indicator, which was developed as part of the operational Global Integrated Drought Monitoring and Prediction System (GIDMaPS, http://drought.eng.uci.edu), is the Multivariate Standardized Drought Index (MSDI, Hao and AghaKouchak, 2013), which is based on a combination of soil moisture and precipitation anomalies through a copula function.

At a European scale, the Combined Drought Indicator (CDI) provides a concise representation of the evolution of agricultural droughts, suitable for communication to both specialized end-users, policy-makers and the general public (Vogt et al., 2018b). The CDI, originally conceived by Sepulcre-Canto et al. (2012), has been successfully applied within the European Drought Observatory (EDO; https://edo.jrc.ec.europa.eu) of the EU's Copernicus Emergency Management Service (https://emergency.copernicus.eu), as part of a near-real time monitoring with dekadal (roughly 10 days, 3 times at month) updates and a time-lag of just a few days.

A similar combining approach, albeit with a strong focus on agricultural production and food security, has been recently implemented as part of the European Commission's Anomaly hot Spots of Agricultural Production (ASAP, https://mars.jrc.ec.europa.eu/asap) system (Rembold et al., 2019).

Other hybrid drought indicators, mostly based on the combination of meteorological soil moisture and streamflow indices via artificial neural networks or entropy theory, were recently

73 introduced in the literature and applied in several regional studies (i.e. Karamoutz et al., 2009;
74 Yang et al., 2014; Zhu et al., 2018).

75 Regarding the CDI, it has proved to be effective at reliably capturing the start and
76 development of most of the severe droughts that affected European countries throughout almost
77 10 years of its operational use in EDO, as documented by the analytical drought reports that are
78 regularly published through the EDO web portal
79 (https://edo.jrc.ec.europa.eu/edov2/php/index.php?id=1051). Maps of EDO's CDI have also been
80 extensively used by the European Commission's Emergency Response Coordination Centre (ERCC),
81 for their daily maps on the most important ongoing emergency events
82 (https://erccportal.jrc.ec.europa.eu/Maps/Daily-maps).

83 While the CDI can claim a considerable number of successful applications in the case of
84 recognized drought events, a day-by-day analysis of its various components has led to an
85 increased understanding of its behaviour, and has also highlighted potential improvements,
86 particularly with regard to its temporal consistency in the case of long-lasting events. The resulting
87 expertise, which is based on extensive practical experience and a long history of actual cases, can
88 be used to improve the indicator's performance in those circumstances where it currently may fall
89 short of expectations. However, given the operational nature of the index, and its reliance on the
90 availability of near real-time input data, changes on the current forcing data are not considered at
91 this stage, since this may require the acquisition of additional datasets not readily available in an
92 operational context. Additionally, any modifications to the modelling framework of an established
93 indicator such as the CDI, must take into account the existing considerable community of users,
94 who are accustomed to the indicator in its current form, as well as its acceptance within the
95 scientific community as a recognized indicator (e.g. Clark et al., 2016; Mariani et al., 2018; WMO
96 and GWP, 2016), as further exemplified by its use in major case-studies and inter-comparison

analyses (e.g. Blauhut et al., 2016; Jiménez-Donaire et al., 2020; Schwarz et al., 2020).

In light of these considerations, the main goal of this paper is to propose a revised version of the CDI, with a focus on improving the overall quality of the indicator's performance without introducing additional or alternative input datasets, and preserving the original modelling concept that has achieved successful results over many documented case studies. To this end, the study compares the performance of the proposed revision of the indicator against the current operational EDO version during some of the main drought events in Europe in the past 20 years. The spatio-temporal characteristics of these droughts were derived from independent data sources, such as yield and impacts databases, and were used as reference to assess the consistency of the model outcomes with the background theoretical framework and the adherence to the observed real drought dynamics.

2. Material and Methods

In this section, the input datasets that are used for computing the CDI are described, and the computation methods that are applied in both the current version and proposed revision of the indicator are outlined. The set of case studies of past drought events used to compare the performances of the current and proposed new versions of the indicator is also described, together with the adopted evaluation strategy.

2.1 Input datasets

The Combined Drought Indicator (CDI) is computed on the basis of the inter-dependency of three main variables: precipitation, soil moisture, and vegetation greenness. The values for each of these quantities are standardized as deviations from historical climatology, and compared with a threshold value to discriminate between normal and extreme conditions. While the data processing approach is conceptually analogous for all three variables, some peculiarities (for

example regarding the data's spatio-temporal resolution and reference baseline) are worth highlighting, and these are described in the following sub-sections.

2.1.1 Precipitation

Monthly precipitation maps at a spatial resolution of 0.25 degrees are derived by blending daily rainfall observations at SYNOP (Surface Synoptic Observations) stations from the MARS database (http://mars.jrc.ec.europa.eu) of the European Commission's Joint Research Centre (JRC), with monthly precipitation maps at a spatial resolution of 1.0 degree from the Global Precipitation Climatology Centre (GPCC, http://gpcp.dwd.de).

The 1-month and 3-month Standardized Precipitation Index (SPI-1 and SPI-3, respectively, McKee et al., 1993) are calculated using the two-parameter gamma distribution fitted over a 30-year reference period (1981-2010) using the maximum likelihood estimators of Thom (1958) and Greenwood and Durand (1960). SPI-3 is selected because of its documented correlation with agricultural drought (WMO, 2012), whereas SPI-1 is selected due to its suitability for detecting the possible occurrence of flash droughts (when combined with increased evaporative demand due to high temperatures, low humidity and/or strong winds), as described by Otkin et al. (2018). In line with Sepulcre-Canto et al. (2012), a threshold value of -1.0 is used for SPI-3, marking the start of moderately dry conditions according to McKee et al. (1993), whereas a threshold value of -2.0 is used for SPI-1, denoting the start of extremely dry conditions.

For computing the CDI, both SPI indicators are used jointly to detect precipitation shortages. Hence, for the sake of simplicity a Boolean SPI indicator (zSPI) is defined, which assumes a value of 1 if either SPI-1 or SPI-3 reports a dry status, as follows:

$$\mathrm{zSPI} = \begin{cases} 1 & \mathrm{SPI\text{-}3} < -1 \quad or \quad \mathrm{SPI\text{-}1} < -2 \\ 0 & otherwise \end{cases} \tag{1}$$

2.1.2 Soil Moisture

The soil moisture anomaly index (zSM) is computed using the modelled soil moisture output of the LISFLOOD hydrological precipitation-runoff model (De Roo et al., 2000). Firstly, dekadal (roughly 10-day) maps of the Soil Moisture Index (SMI; Seneviratne et al., 2010) are computed at a spatial resolution of 5 km, as a weighted average of the daily volumetric soil moisture values produced by LISFLOOD for the skin and root zone layers. Successively, the zSM is computed as standardized deviations (i.e. z-scores) of the values from the full available period (1995-2018).

In the present study, SMI replaces the soil suction (pF) that was previously used both within EDO and for the original development of the CDI. This has been done as part of a reorganization of the EDO data portal, in order to improve the readability of maps for non-expert users, given that SMI simply ranges from 0 (dry) to 1 (wet). Since both SMI and pF are derived from the same daily volumetric soil moisture dataset and using the same pedotransfer function (PTF; Laguardia and Niemeyer, 2008), the obtained zSM maps are in practical terms the opposite of the Anomaly pF used in Sepulcre-Canto et al. (2012). Following these considerations, a threshold of -1 is adopted to discriminate dry conditions in zSM, analogously to what is used for SPI-3.

2.1.3 Vegetation greenness

In this study, the biophysical variable Fraction of Absorbed Photosynthetically Active Radiation (FAPAR), which is estimated from satellite remote sensing data, is used as a proxy for the health status of vegetation. Sepulcre-Canto et al. (2012) adopted the 10-day composite FAPAR images provided by the European Space Agency (ESA), derived from the Medium Resolution Imaging Spectrometer (MERIS) on board of the ENVISAT platform. Following the failure of ENVISAT in 2012, the MOD15A2H Collection 6 FAPAR product (Myneni, 2015), as derived from the Moderate-Resolution Imaging Spectroradiometer (MODIS) sensor on board of the Terra satellite, has been used as a replacement in the operational implementation of the CDI.

The MOD15A2H product is provided by the US National Aeronautics and Space Administration (NASA) at spatial resolution of 500 metres, as 8-day maximum composites. Within EDO, these raw data are re-projected onto a 0.01 degrees latitude / longitude regular grid, and dekadal maps are derived by means of a weighted average of the two closest 8-day maps followed by an exponential smoothing (Cammalleri et al., 2019). As in the case for soil moisture, anomalies of FAPAR (zFAPAR) are computed as a standardized z-score on the full available dataset baseline period (2001-2018). Also here, a threshold value of -1.0 is adopted to highlight dry conditions.

2.2 The current version of CDI, as implemented in EDO (CDI-v1)

As is described in detail by Sepulcre-Canto et al. (2012), in the modelling framework of the CDI the evolution of a drought event is conceptualized by a cause-effect relationship, assuming that a shortage in precipitation leads to a soil moisture deficit, culminating in reduced vegetation productivity. In its original form, data for the variables zSPI, zSM and zFAPAR (see above) are used to characterize three stages of an idealized agricultural drought:

- WATCH, in which the precipitation is below normal (zSPI = 1), and an early warning signal of a potential drought affecting agriculture can be observed.
- WARNING, when a precipitation deficit propagates in the hydrological cycle and affects soil water content (zSPI = 1 & zSM < -1).
- ALERT, when the effects of drought become visible as vegetation stress (zSPI = 1 & zFAPAR < -1).

During the operational implementation of the indicator, two additional recovery stages were introduced (see https://edo.jrc.ec.europa.eu/factsheets), aimed at better capturing the fade-out phase of a drought, namely the PARTIAL RECOVERY and FULL RECOVERY stages. In both stages, the previous month's zSPI ($zSPI_{m-1}$) is introduced to account for the preceding conditions:

- PARTIAL RECOVERY: zSPI returns to normal values even if vegetation is still negatively affected ($zSPI_{m-1}$ = 1 & zSPI = 0 & zFAPAR < -1).
- FULL RECOVERY: Both precipitation and FAPAR return to normal conditions ($zSPI_{m-1}$ = 1 & zSPI = 0 & zFAPAR $\geq$ -1).

This operational implementation of the index is the one commonly referred to in the scientific and technical drought literature when CDI is described.

The CDI modelling framework described above is summarised in Fig. 1, where the different stages of CDI (from WATCH to FULL RECOVERY) are depicted according to the eight cases that can be obtained by combining the two possible binary states for each of the three main variables (zSPI, zSM, zFAPAR), as well as a function of $zSPI_{m-1}$.

Due to its operational status, the maps of the CDI that are currently available in EDO are always processed using data available up to the release date of a new map. For this reason, some inconsistencies in the reference baseline and actual data (e.g. FAPAR data source) are present in this operational dataset. For the present study, a self-consistent dataset has been produced by re-computing the CDI with the best data available at the end of 2018. This dataset (referred to here as CDI-v1) consists of 648 dekadal maps at 5-km spatial resolution, from January 2001 to December 2018. In order to compute the CDI at this spatial resolution, the original data for zSPI and zFAPAR were initially resampled over the zSM grid, using the nearest neighbour and spatial average procedure, respectively.

2.3 The revised version of CDI proposed here (CDI-v2)

In order to better understand the modifications to the CDI that are proposed here, two case studies where CDI-v1 was not able to capture in full the evolution of the drought, are first reported.

213 The original concept behind the CDI assumes the sequential occurrence of extreme
214 conditions detected by the three constituent indicators (i.e. SPI, soil moisture anomalies, and
215 FAPAR anomalies). In fact, while Sepulcre-Canto et al. (2012) illustrated the CDI scheme as a
216 cascade process (see the schematisation in that paper's Fig. 1), its actual implementation can be
217 seen more in the context of a nested approach, since each successive stage is contained within the
218 definition of the previous one. This is exemplified by the inclusive nature of the calculation (see
219 above, where "&" is used in the definition of the classes). This approach can lead to abrupt breaks
220 in tracking a drought event, when a substantial temporal shift among the three quantities can be
221 observed.

222 For example, the plots in Fig. 2 report the time series of SPI-3 (upper panel), zSM (middle
223 panel) and zFAPAR (lower panel) for a year that includes a drought event in Spain. Dotted vertical
224 lines demarcate the full span of the drought event. At the top of each plot, a box demarcates the
225 period when the stage-specific conditions for WATCH, WARNING and ALERT are met. By an *a*
226 *posteriori* analysis of the event, it is easy to assess a desirable sequence of stages for each dekad,
227 as reported in the bottom part of the lower plot (i.e. the ideal outcome of a revised CDI, ideally
228 CDI-v2). However, from the actual sequence of CDI values (CDI-v1) it can be seen that the event is
229 interrupted in the middle of the soil moisture deficit period due to the return of precipitation to
230 normal conditions.

231 A second example is shown in Fig. 3 for a drought event in France, where the time series of
232 SPI-3, zSM and zFAPAR suggest an extensive period of soil moisture deficit following a
233 precipitation deficit, which caused a short period of FAPAR anomalies. Even if two periods meeting
234 the requirement for a WARNING and an ALERT status are observed (see boxes at the top of the
235 middle and lower panels, respectively), a temporary return above the thresholds is observed (for
236 one or two dekads) in both zSM and zFAPAR time series. In an *a posteriori* analysis, a single

continuous ALERT period would have been likely detected (see ideal CDI sequence at the bottom of Fig. 3). CDI-v1 instead treats those gaps as interruptions, causing a back-and-forth transition between the ALERT and WARNING stages.

This behaviour is in contrast to the cause-effect principle on which the indicator is based, and even if this occurrence cannot be always avoided in real case studies, it should be kept to a minimum. It is worth noting how, also in this second case, according to CDI-v1 the event stops well before the end of the soil moisture deficit, due to the return of precipitation to normal conditions (SPI-3 > -1).

The two examples reported above highlight the main drawbacks of the current operational version of the CDI, which can be summarized as follow:

- Lack of a proper cascade process in favour of a nested approach, which can cause an early interruption in drought events in case of notable shifts between time series.
- Absence of a check for possible small gaps within a stage, which can lead to inconsistencies in the temporal sequence and quick alternation of different stages.

The revised version of the CDI that is proposed here (i.e. hereafter called CDI-v2) addresses these two key issues by introducing two principal modifications:

- Set-up of different rules to ensure temporal continuity based on the previous dekad's CDI (CDI_{d-1}) rather than the preceding SPI (SPI_{m-1}).
- Addition of a second set of threshold values to detect both temporary gaps within a stage, and the fade-out phase of a drought.

These modifications are implemented according to the scheme depicted in Fig. 4, where the upper part of the Table is analogous to that of Fig. 1, while the lower part details the values assumed by the index for all the possible cases of preceding CDI values.

By juxtaposing Figs. 1 and 4, it is possible to highlight the main changes introduced after discriminating the outputs on the basis of CDI_{d-1}. On the one hand, it is possible to notice how CDI-v2 (i.e. the proposed revision) behaves identically to CDI-v1 (i.e. the current version) at the start of a new event (first row, CDI_{d-1} = 0 or 4). On the other hand, for an on-going event (CDI_{d-1} = 1,2,5,3,6), CDI-v2 still behaves similarly to CDI-v1 for the combinations *a*-*b* and *f*-*h*, whereas some major differences can be observed for the cases *c*-*e*. In these latter instances, both the WARNING and ALERT stages are preserved if zSM and zFAPAR values support these conditions independently from the value of zSPI. This modification aims at solving the problem highlighted by the example in Fig. 2.

The lower part of the table in Fig. 4 highlights how the inclusion of a second threshold for zSM and zFAPAR (i.e. 0.0 in both cases) aims at addressing those situations when the CDI tends to return to a stage that conceptually precedes that of the previous dekad (i.e. a WARNING following an ALERT). In all these circumstances, two TEMPORARY RECOVERY stages are introduced - one for soil moisture and one for FAPAR - if the values of zSM or zFAPAR fall between the two threshold values (i.e. -1.0 and 0.0). Since these classes are meant to be temporary, we wish to avoid that the index remains locked in these classes for long periods. For this reason, a constraint on the maximum duration of the TEMPORARY RECOVERY stages is fixed at 4 dekads. This value is chosen as the minimum length to ensure the inclusion of two consecutive monthly zSPI values.

2.4 Past drought events

In absence of a reliable independent benchmark for the evaluation of the CDI behaviour, the performance of the proposed revision of the CDI (CDI-v2 in this paper) is compared against the current version of the index (called CDI-v1) over selected past drought events in Europe occurring during the period 2001-2018 (years when all the input datasets are overlapping).

Several drought events of different extent and severity were observed during the reference

284 period, including the three large-scale and renowned events of 2003 in central Europe (Rebetez et
285 al., 2006), 2005 in Iberia Peninsula (Garcia-Herrera et al., 2007) and 2018 in northern Europe
286 (Buras et al., 2019). Other documented events at national / regional scale include the droughts in
287 Italy and Romania in 2007, western Germany / France in 2011, Romania and Portugal in 2012,
288 eastern Spain in 2014, eastern France / western Germany in 2015 and central Italy in 2017.

289 For these events, the improvement in the coherence between the proposed revision of the
290 index and the CDI theoretical modelling framework is firstly verified for two test datasets of
291 locations where the operational CDI-v1 was successfully validated in the past. The first dataset of
292 locations corresponds to drought events that were originally used by Sepulcre-Canto et al. (2012)
293 to validate the index. These include data from: Magdeburg (DE), Ciampino (IT) and Wattisham (UK)
294 during the 2003 drought; Albacete (ES) and Beja (PT) in 2005-2004; Ciampino (IT) for the drought
295 in 2007; and Magdeburg (DE) and Deols (FR) during 2011.

296 The second dataset of locations is derived from the droughts documented in the reports
297 produced by EDO (https://edo.jrc.ec.europa.eu/edov2/php/index.php?id=1051) since the CDI's
298 operational implementation. These include data from: Lisbon (PT) in 2012; Valencia (ES) for the
299 2014 drought; Strasbourg (FR) in 2015; Rome (IT) during summer 2017; and Dublin (IE), Hannover
300 (DE), Poznan (PL) and Silkeborg (DK) for the drought in 2018.

301 This qualitative analysis over selected test sites is complemented by a quantitative analysis
302 on the full dataset that evaluates the frequency in which each cell experiences a stage sequencing
303 in contrast with the assumed cause-effect modelling (i.e. a dekad with WARNING followed by one
304 with WATCH), providing a metric to quantify the improvements associated with the proposed
305 revision.

306 **2.5 Evaluation strategy**

307 Long records of yield data for cereals (including rice) from the EUROSTAT database were used to

detect specific regions with documented drought impacts in agriculture during the above-reported drought years. Even if it was not possible to extract evidence of drought impacts for all the events, mainly due to gaps in data records, six regions were detected from the above-mentioned drought years, as summarized in Table 1. The reported yield data show how the production was lower than the long-term average yield for all the regions, as they were actually the minimum in the records for all the cases, the only exception being ES62, Region of Murcia (which recorded the second to last yield in 2014 only after 2005).

Assuming that the reduction in yield is a measure of the impacts of drought over vegetated land, statistics of the ALERT stage in these EUROSTAT NUTS (Nomenclature of Territorial Units for Statistics) regions during the drought events were investigated as a means of quantifying the effects of the proposed modification of the CDI. The duration of the drought according to the CDI is quantified as the period when the percentage of NUTS with WATCH+WARNING+ALERT is at least 20%, and within this period the average percentage of area under ALERT (P_{ALERT}) and the maximum modelled ALERT percentage in the same period (M_{ALERT}) are computed for the two CDI versions, assuming that high values in both P_{ALERT} and M_{ALERT} are expected in these study cases given the observed drastic reduction in yield.

3. Results and Discussion

3.1 Temporal consistency of drought stages

Following the modification introduced, one of the main improvements that may be expected in the revised version of the CDI (CDI-v2) concerns the temporal consistency at the local scale. For this reason, an initial test was made to compare the temporal behaviour of the current version (CDI-v1) and proposed revision (CDI-v2) of the indicator, over selected locations in Europe, during well-documented drought events.

The plots in Figs. 5 and 6 show dekadal time series of CDI-v1 (upper line) and CDI-v2 (lower line), with the colours corresponding to the classifications in Figs. 1 and 4, respectively. The sites in Fig. 5 correspond to the locations used for validation by Sepulcre-Canto et al. (2012), whereas the sites in Fig. 6 were extrapolated from the EDO reports for the most recent drought events.

In all the sites, the start of the drought event coincides for the two versions of the indicator (CDI-v1 and CDI-v2), as is to be expected given the analogous conditions adopted to define a new event. Over some sites, the two versions do not differ substantially, as in the case of Wattisham and Magdeburg (Fig. 5), and Silkeborg and Poznan (Fig. 6), where only minor signs of the issues highlighted in Figs. 2 and 3 can be observed. In those study sites, the temporal evolution of the droughts appears to be well reproduced by both versions of the indicator, with the start-, peak- and end-dates consistent with the scientific literature for the events (Buras et al., 2020; Ciais et al., 2005; Hanel et al., 2018; Rebetez et al., 2006).

Conversely, the drought development for the sites of Albacete (2005 drought), Ciampino (2007 drought), Lisbon (2012 drought) and Valencia (2014 drought), differs substantially for the revised version (CDI-v2) compared with the current version (CDI-v1), with an overall longer duration and prolonged periods under the WARNING and ALERT stages. The drought events at those sites are rather similar to what is depicted in Fig. 2, with a long period of soil water deficit and plant water stress during the whole dry season following a rainfall deficit early in spring and a hot and dry summers. In these cases, the new version of the index appears to be capable to capture those instances when a drought is prolonged by higher than normal evaporative demand even after the rainfall returns to normal. Considering the well documented severity of those droughts (Garcia-Herrera et al., 2007; MeteoAM, 2007; Spinoni et al., 2015), the behaviour of CDI-v2 seems to be much more in line with the expected evolution of the droughts.

Finally, for some study cases - specifically Deols (2011 drought), Strasbourg (2015 drought)

and Dublin (2018 drought) - the erratic behaviour of CDI-v1 that is evident later in the event (similar to the example of Fig. 3), is replaced by a noticeably smoother dynamic in CDI-v2, which is more in line with both the desirable sequencing of stages and the expected behaviour of a slow-evolving phenomenon such as drought.

For most of the test sites, the representation of the temporal evolution of the drought events by CDI-v2 better fits the conceptual "cause-effect" framework of the indicator, by reducing inconsistent changes in the drought stages. This is quantified by the data reported in Table 2, where the percentage of cells experiencing one of the three major unexpected stage sequencing is reported, specifically: i) WATCH following a WARNING, ii) WATCH following an ALERT, or iii) WARNING following an ALERT. In all three cases the results, expressed as an average percentage of the area affected by drought (i.e. the sum of all stages excluding FULL RECOVERY), show a drastic decrease when the CDI-v2 is used instead of CDI-v1. While the reduction occurs for all the three conditions considered, major improvements can be observed in the reduction of the instances when a WARNING is followed by a WATCH (4.25% for CDI-v1 compared with 0.88% for CDI-v2). Overall, the total percentage of inconsistent sequencing is reduced from about 7% for CDI-v1 to just 2% for CDI-v2, supporting the assumption that the revised indicator (CDI-v2) better captures the expected evolution of the droughts compared to the current version (CDI-v1) by minimizing the unexpected behaviours.

The data in Table 3 summarize some key statistics of the ALERT stage over the areas where significant impact in agricultural production (i.e. yield) were recorded during past droughts (see Table 1). Overall, both P_{ALERT} and M_{ALERT} are higher for CDI-v2 compared with CDI-v1, with P_{ALERT} being more than double and M_{ALERT} about 30% higher on average for CDI-v2, with the highest values observed for the two case studies in Spain and the lowest over Sweden in 2018. Given the severe impact of drought over these regions, documented by the concurrent reduced yield

recorded (see Table 1), the large presence of ALERT conditions reported by the CDI-v2 is more in line with the expected severity of the drought event according to the CDI conceptual modelling framework.

3.2 Analysis during major drought events

An analysis of the full spatio-temporal evolution of the drought events based on the current (CDI-v1) and revised (CDI-v2) versions of the CDI indicator is performed for the three largest droughts, as summarised in Figs. 7 to 9 for central Europe (2003), the Iberian Peninsula (2005), and northern Europe (2018). In each case, the upper plot shows the percentage of the area affected by drought (i.e. the sum of all stages excluding FULL RECOVERY) for each month, whereas the maps show examples of the CDI's spatial distribution for selected dekads during the event (as demarcated by squares on the upper-plot's X-axis).

In all these study cases, it is evident how the percentage of the area that is considered under drought has a similar temporal behaviour for the two (current and revised) versions of the indicator, with the latter having only a slightly larger spatial coverage later in the events. An examination of the maps, however, shows that even if the total area affected is similar, the partitioning among the different stages may drastically differ around the peak of the drought. Indeed, the maps for CDI-v1 and CDI-v2 look quite similar at the beginning of the events, but in the case of CDI-v2 these become much more uniform, and with a higher number of cells under the ALERT stage, later in the event. The larger number of ALERT in CDI-v2 is more in line with the conceptualized behaviour of the index, which should reach the ALERT stage at the peak of the drought development in the case of severe droughts.

The overall dynamic of the 2003 drought (Fig. 7) depicted by the two version of the index is in line with the historical reconstruction of the event made by the European Drought Impact Inventory (EDII) and the European Drought Reference (EDR) database

(https://www.geo.uio.no/edc/droughtdb). According to EDII, the event started around April 2003 with a main incidence for eastern Europe up to early June, followed by a propagation through central Europe and its peak in late August, before ending in November 2003. However, some key differences in favour of the proposed revision of the index can be observed, such as the higher and more realistic fraction of areas under ALERT status, which can be seen in the CDI-v2 compared with CDI-v1 during the drought peak (last map of the series in Fig. 7), against the FULL RECOVERY areas modelled by CDI-v1 during the expansion of the event in June.

Similarly, the drought event of 2005 over the Iberia Peninsula (Fig. 8) seems to be well reproduced by both indices. Based on EDII and EDR, the drought in 2005 was part of a longer drought between autumn / winter 2004 and summer 2006. The event stated in the west, already in late 2004, mainly over Portugal, and reached its full extent between July and October 2005, with a secondary wave observed in summer 2006. The latter was due to the residual deficit that followed the extremely hot and dry summer of 2005.

This dynamic is well depicted by the plot in Fig. 8 (upper panel), with an already significant fraction of area under drought at the start of 2005 (about 20% and 30%, according to CDI-v1 and CDI-v2, respectively) mostly located over Portugal (see the first map of the series in January 2005). Peak extension is reached in July for the CDI-v1 and between August and September for the CDI-v2, followed by a slow decline that left still a significant area under drought entering 2006, especially in the case of CDI-v2. Even if the depiction of the event is quite similar in the first half of the year (i.e. first three maps of the series), in some circumstances (e.g. between July and August) the current version (CDI-v1) shows rather different patterns for two consecutive dekads, whereas the revised version (CDI-v2) gives more temporally consistent outcomes, especially when comparing maps in succession.

The drought event of 2018 (Fig. 9) was characterized by an extremely warm but not

exceptionally dry spring, that rapidly became an extended and persistent summer drought, due to the extreme record-breaking temperatures (Peters et al., 2020). This behaviour is well depicted by both versions of the CDI, with a sudden start between April and June (area under drought jumping from 0% to 80%) and a quite widespread and enduring drought between July and October. In this study case, less discrepancies can be observed between the behaviour of the two versions of the index, compared with the previous two droughts. The most notable difference is the abrupt stop of drought conditions in Sweden around the peak of the event for CDI-v1 (see last two images of the series in September and October).

Overall, the analysis of the spatial patterns of both CDI versions during these three major drought events reveals a more stable behaviour for CDI-v2 compared with CDI-v1. In order to provide a quantitative estimation of the effects of the proposed changes to the partitioning of drought stages during an event, the plots of Fig. 10 show the time series of the percentage differences between CDI-v1 and CDI-v2, in the fraction of the area in the WATCH, WARNING and ALERT stages, for the same three main droughts that are depicted in Figs. 7-9. Those plots show no substantial differences at the beginning of each event (first 2-3 months, changes < 5%), and a reduction in the WATCH fraction for CDI-v2 (negative differences) in favour of an increase in the WARNING and ALERT fractions during the development of the events. The results are consistent across the three study cases, suggesting that the revised version of the indicator (CDI-v2) better reflects the "cause-effect" principle, by showing a progressive propagation of the drought from one stage to the next. For example, in Fig. 10, some areas that are classified as WATCH by CDI-v1 in a late phase of the events, are marked as WARNING and ALERT by CDI-v2, with an increased percentage of WARNING preceding the peak of the drought (June-July in 2003, and May-June in 2018), and an increased percentage of ALERT at the peak of the event (September in 2003 and 2018; and August-September in 2005).

452 It is worth noting that even if some of the largest percentage changes from WATCH to ALERT
453 occur later in the event (i.e. in autumn after the peak), this is not accompanied by a larger drought
454 area, as shown by the upper plots of Figs. 7-9. In fact, after the drought has reached its peak, CDI-
455 v2 depicts an affected area that is reduced in size but mostly constituted by ALERT, whereas in the
456 previous version WATCH conditions were still reported towards the end of the event.
457

458 ## 4. Summary and Conclusions

459 A revised version of the Combined Drought Indicator (CDI), which is currently implemented
460 operationally within the European Commission's European Drought Observatory (EDO) for
461 providing early warning and monitoring of agricultural droughts, has been analysed. The proposed
462 revision of the CDI is based on the extensive experience that has been gained from applying the
463 indicator during several major drought events that have affected different parts of Europe over
464 the last ten years.

465 While the current version of the CDI (called CDI-v1 in this paper) has successfully captured
466 the onset of most of the documented major drought events, its ability to track correctly the
467 evolution of events has been limited in the case of long lasting droughts, with significant temporal
468 shift between reduced rainfall, soil moisture deficit and vegetation stress periods caused by high
469 temperature and evaporative demand following the rainfall deficit. The proposed revision of the
470 CDI (called CDI-v2 in this paper) aims at addressing those shortcomings, without either modifying
471 the required input data or substantially altering the conceptual "cause-effect" framework
472 underlying its original development, especially given the indicator's proven reliability based on
473 many case studies and inter-comparison analyses. This enables the retroactive application of the
474 revised indicator to past drought events, without the need for additional inputs or changes in the
475 underlying datasets. For similar reasons, the three main stages of drought (i.e. WATCH, WARNING

476 and ALERT), which were originally defined in Sepulcre-Canto et al. (2012), remain unchanged, as
477 does the inclusion of a FULL RECOVERY stage to identify the end of a drought period and the
478 return to normal conditions.

479 The two main changes that are introduced in the CDI-v2 are:

480 • The inclusion of a constraint on the temporal consistency, based on the CDI's value in the
481 preceding dekad (thus rendering obsolete the previously defined PARTIAL RECOVERY stage).

482 • The addition of two TEMPORARY RECOVERY stages - one for soil moisture and the other for
483 vegetation greenness (represented by FAPAR) - with the aim of improving temporal continuity in
484 the case of small gaps in the middle of periods that are otherwise characterised by the same
485 drought stage.

486 A comparison of the performance of the current version (CDI-v1) and proposed revision
487 (CDI-v2) of the indicator highlights the capability of CDI-v2 to improve on the results of CDI-v1 in
488 several circumstances, without impairing the overall performance for drought events that are
489 already correctly reproduced by CDI-v1. This is indicated by the reduced number of instances
490 where a specific stage is followed by another that is not coherent with the cause-effect modelling
491 framework, as well as by the increase in the extension of ALERT areas (i.e. visible vegetation
492 stress) during events with recorded impacts in agricultural production quantified by reduced
493 annual yield.

494 While for a few test cases (e.g. the 2018 drought in northern Europe) only marginal changes
495 are observed, in the majority of the cases the new version of the indicator (CDI-v2) clearly
496 outperforms the current version, with an overall better temporal consistency and a more
497 continuous sequencing of the drought stages. In all the observed study cases, the CDI-v2 returns a
498 reduced number of cells under WATCH around the peak of the drought in favour of WARNING
499 (before the peak) and ALERT (at the peak) stages.

On a general level, it is clear that the new version of the indicator better approximates the expected spatio-temporal characteristics of a drought event in all the performed analyses, with a more realistic succession of the WATCH, WARNING and ALERT stages, and a large spatial consistency in the modelled patterns. In addition, in spite of the improved performance of the revised version of the CDI, the indicator's "look and feel" are not substantially altered. Given the well established community of users of the current version of the CDI that is implemented in EDO, this is a key consideration that can ensure a smooth future transition to the operational use within EDO of the revised version of the CDI that is proposed here.

Finally, with regard to potential further developments of the methodology, in the framework of the continuous maintenance of the EDO system additional analyses shall be carried out in order to evaluate the potential integration of other indicators, aimed at better capturing drought events at different time scales (e.g. indices based on ground water), or to incorporate also information on evaporative demand into the modelling of meteorological conditions.

References

Blauhut, V., Stahl, K., Stagge, J.H., Tallaksen, L.M., De Stefano, L., and Vogt, J.: Estimating drought risk across Europe from reported drought impacts, drought indices, and vulnerability factors, Hydrol. Earth Syst. Sci., 20, 2779-2800, doi:10.5194/hess-20-2779-2016, 2016.

Buras, A., Rammig, A., and Zang, C.S.: Quantifying impacts of the drought 2018 on European ecosystems in comparison to 2003, Biogeosciences, 17, 1655-1672, doi:10.5194/bg-17-1655-2020, 2020.

Cammalleri, C., Verger, A., Lacaze, R., and Vogt, J.V.: Harmonization of GEOV2 FAPAR time series through MODIS data for global drought monitoring, Int. J. Appl. Earth Obs. Geoinf., 80, 1-12, doi:10.1016/j.jag.2019.03.017, 2019.

Ciais, P., Reichstein, M., Viovy, N., Granier, A., Ogée, J., Allard, V., Aubinet, M., Buchmann, N., Bernhofer, C., Carrara, A., Chevallier, F., De Noblet, N., Friend, A.D., Friedlingstein, P., Grünwald, T., Heinesch, B., Keronen, P., Knohl, A., Krinner, G., Loustau, D., Manca, G., Matteucci, G., Miglietta, F., Ourcival, J.M., Papale, D., Pilegaard, K., Rambal, S., Seufeet, G., Soussana, J.F., Sanz, M.J., Schulze, E.D., Vesala, T., and Valentini, R.: Europe-wide reduction in primary productivity caused by the heat and drought in 2003, Nature, 437, 529-533, doi:10.1038/nature03972, 2005.

Clark, A., McGowen, I., Crean, J., Kelly, R., and Wang, B.: Stage 1 – Enhanced Drought Information System: NSW DPI Combined Drought Indicator. Technical Report, NSW Department of Primary Industries, ISBN 978-1-76058-016-2, 76 pp, 2016.

De Roo, A., Wesseling, C., and Van Deursen, W.: Physically based river basin modeling within a GIS: The LISFLOOD model, Hydrol. Process., 14, 1981-1992, doi:10.1002/1099-1085(20000815/30)14:11/12<1981::AID-HYP49>3.0.CO;2-F, 2000.

Garcia-Herrera, R., Paredes, D., Trigo, R.M., Trigo, I.F., Hernandez, H., Barriopedro, D., and

537 Mendes, M.T.: The outstanding 2004-2005 drought in the Iberian Peninsula: associated
538 atmospheric circulation, J. Hydrometeorol., 8, 483–498, doi:10.1175/JHM578.1, 2007.
539 Greenwood, J.A., and Durand, D.: Aids for fitting the gamma distribution by maximum likelihood,
540 Technometrics, 2, 55-65, doi:10.1080/00401706.1960.10489880, 1960.
541 Hanel, M., Rakovec, O., Markonis, Y., Máca, P., Samaniego, L., Kyselý, J., and Kumar, R.: Revisiting
542 the recent European droughts from a long-term perspective, Sci. Rep., 8, 9499,
543 doi:10.1038/s41598-018-27464-4, 2018.
544 Hao, Z., and AghaKouchak, A.: Multivariate Standardized Drought Index: a multi-index parametric
545 approach for drought analysis. Adv. Water Resour., 57, 12-18,
546 doi:10.1016/j.advwatres.2013.03.009, 2013.
547 Karamoutz, M., Rasouli, K., and Nazif, S.: Development of a hybrid index for drought prediction:
548 Case study, J. Hydrol. Eng., 14(6), doi:10.1061/(ASCE)HE.1943-5584.0000022, 2009.
549 Laguardia, G., and Niemeyer, S.: On the comparison between the LISFLOOD modeled and the
550 ERS/ASCAT derived soil moisture estimates, Hydrol. Earth Syst. Sci., 12, 1339-1351,
551 doi:10.5194/hess-12-1339-2008, 2008.
552 Jiménez-Donaire, M., Tarquis, A., and Giráldez, J.V.: Evaluation of a combined drought indicator
553 and its potential for agricultural drought prediction in southern Spain, Nat. Hazards Earth
554 Syst. Sci., 20, 21-33, doi:10.5194/nhess-20-21-2020, 2020.
555 Mariani, S., Braca, G., Romano, E., Lastoria, B., and Bussettini, M.: Linee Guida sugli Indicatori di
556 Siccità e Scarsità Idrica da utilizzare nelle attività degli Osservatori Permanenti per gli Utilizzi
557 Idrici - Stato Attuale e Prospettive Future (in Italian), Technical Report, CREiAMO PA, 56 pp.,
558 2018.
559 McKee, T.B., Doesken, N.J., and Kleist, J.: The relationship of drought frequency and duration to
560 time scales, in: Proceedings of the 8th Conference of Applied Climatology, Anaheim, CA, Am.
561 Meteorol. Soc. 179-184, 1993.

562 MeteoAM: Climatologia – temperatura e precipitazioni Aprile 2007, available at:
563 http://clima.meteoam.it/bollettinoMensile.php, last access: 10 March 2020, 2007.
564 Myneni, R.B.: MOD15A2H MODIS/Terra leaf area Index/FPAR 8-Day L4 global 500m SIN grid V006.
565 NASA EOSDIS Land Processes DAAC, doi:10.5067/modis/mod15a2h.006, 2015.
566 Otkin, J.A., Svoboda, M., Hunt, E.D., Ford, T.W., Anderson, M.C., Hain, C., and Basara, J.B.: Flash
567 droughts: A review and assessment of the challenges imposed by rapid-onset droughts in the
568 United States, Bull. Amer. Meteor. Soc., 99, 911-919, doi:10.1175/BAMS-D-17-0149.1, 2018.
569 Peters, W., Bastos, A., Ciais, P., and Vermeulen, A.: A historical, geographical and ecological
570 perspective on the 2018 European summer drought, Phil. Trans. R. Soc. B, 375, 20190505,
571 doi:10.1098/rstb.2019.0505, 2020.
572 Pischke, F., and Stefanski, R.: Integrated Drought Management Initiatives, in: Wilhite D.A. and
573 Pulwarty R.S. (Eds.). Drought and Water Crises: Integrating Science, Management and Policy
574 (Chapter 3), CRC Press (Taylor & Francis), Boca Raton, 39-54, 2018.
575 Rebetez, M., Mayer, H., Dupont, O., Schindler, D., Gartner, K., Kropp, J.P., and Menzel, A.: Heat
576 and drought 2003 in Europe: A climate synthesis, Ann. For. Sci., 63, 569-577,
577 doi:10.1051/forest:2006043, 2006.
578 Rembold, F., Meroni, M., Urbano, F., Csak, G., Kerdiles, H., Perez-Hoyos, A., Lemoine, G., Leo, O.,
579 and Negre, T.: ASAP: A new global early warning system to detect anomaly hot spots of
580 agricultural production for food security analysis, Agr. Syst., 168, 247-257, doi:
581 10.1016/j.agsy.2018.07.002, 2019.
582 Schwarz, M., Landmann, T., Cornish, N., Wetzel, K.-F., Siebert, S., and Franke, J.: A spatially
583 transferable drought hazard and drought risk modeling approach based on remote sensing
584 data, Remote Sens., 12(2), 237, doi:10.3390/rs12020237, 2020.
585 Sepulcre-Canto, G., Horion, S., Singleton, A., Carrao, H., and Vogt, J.V.: Development of a
586 Combined Drought Indicator to detect agricultural drought in Europe, Nat. Hazards Earth

587 Syst. Sci., 12, 3519-3531, doi:10.5194/nhess-12-3519-2012, 2012.
588 Spinoni, J., Naumann, G., Vogt, J.V., and Barbosa, P.: The biggest drought events in Europe from
589 1950 to 2012, J. Hydrol. Regional Studies, 3, 509-524, doi:10.1016/j.ejrh.2015.01.001, 2015.
590 Svoboda, M., D. Lecomte, M. Hayes, R. Heim, K. Gleason, J. Angel, B. Rippey, R. Tinker, M. Palecki,
591 D. Stooksbury, D. Miskus, and Stephens, S.: The drought monitor. Bull. Amer. Meteor. Soc.,
592 83(8), 1181-1190, doi: 10.1175/1520-0477-83.8.1181, 2002.
593 Thom, H.C.S.: A note on the Gamma distribution, Monthly Weather Rev., 86(4), 117-122,
594 doi:10.1175/1520-0493(1958)086<0117:ANOTGD>2.0.CO;2, 1958.
595 Vogt, J.V., Naumann, G., Masante, D., Spinoni, J., Cammalleri, C., Erian, W., Pischke, F., Pulwarty,
596 R., and Barbosa, P.: Drought Risk Assessment and Management: A Conceptual Framework.
597 JRC Technical Reports, EUR 29464 EN, Publication Office of the European Union, Luxemburg,
598 doi:10.2760/919458, 2018a.
599 Vogt, J.V., Barbosa, P., Cammalleri, C., Carrão, H., and Lavaysse, C.: Drought Risk Management:
600 Needs and Experiences in Europe, in: Wilhite, D.A. and Pulwarty, R.S. (Eds.). Drought and
601 Water Crises. Integrating Science, Management, and Policy (Chapter 18). CRC Press (Taylor &
602 Francis), Boca Raton, 385-407, 2018b.
603 Wilhite, D.A., and Pulwarty, R.S.: Drought and Water Crises: Lessons learned and the road ahead,
604 in: Wilhite, D.A. (Eds.). Drought and Water Crises: Science, Technology, and Management
605 Issue (Chapter 15). CRC Press (Taylor & Francis), Boca Raton, 389-398, 2005.
606 World Meteorological Organization (WMO): Standardized Precipitation Index User Guide (M.
607 Svoboda, M. Hayes and D. Wood), WMO-No. 1090, Geneva, Switzerland, 16 pp, 2012.
608 World Meteorological Organization (WMO), and Global Water Partnership (GWP): National
609 Drought Management Policy Guidelines - A Template for Action. (D.A. Wilhite). Integrated
610 Drought Management Programme (IDMP) Tools and Guidelines Series 1. WMO, Geneva,
611 Switzerland and GWP, Stockholm, Sweden. ISBN: 978-92-63-11164-7 and 978-91-87823-03-

9. 2014.

World Meteorological Organization (WMO), and Global Water Partnership (GWP): Handbook of Drought Indicators and Indices (M. Svoboda and B.A. Fuchs). Integrated Drought Management Programme (IDMP), Integrated Drought Management Tools and Guidelines, Series 2, Geneva, Switzerland, 45 pp, 2016.

Yang, T., Zhou, X., Yu, Z., Krysanova, V., and Wang, B.: Drought projection based on a hybrid drought index using Artificial Neural Networks, Hydrol. Process., 29(11), 2635-2648, doi:10.1002/hyp.10394, 2014.

Zhu, J., Zhou, L., and Huang, S.: A hybrid drought index combining meteorological, hydrological, and agricultural information based on the entropy weight theory, Arab. J. Geosci., 11, 91, doi: 10.1007/s12517-018-3438-1, 2018.

Table 1. Cereals (including rice) yield (t/ha) data for different NUTS regions as derived from the EUROSTAT database. The column "avg. 2000-2018" reports the average yield during the whole period, whereas the column "drought year" reports the actual yield for the drought year specified in the "year" column.

NUTS	Name	year	yield (t/ha)	
			avg. 2000-2018	drought year
DE1	Baden-Württemberg	2003	6.8	5.7
ES42	Castile – La Mancha	2005	2.7	1.3
RO31	Sud – Muntenia	2007	3.5	2.3
RO12	Centru	2012	3.4	1.1
ES62	Region of Murcia	2014	1.1	0.5
SE21	Småland	2018	4.3	2.9

Table 2. Average percentage of cells in drought areas with sequencing in contrast with the "cause-effect" relationship for the full European domain.

Version	WARNING to WATCH	ALERT to WATCH	ALERT to WARNING
CDI-v1	4.25	1.79	1.20
CDI-v2	0.88	0.52	0.82

Table 3. ALERT stage statistics over the NUTS regions with observed yield impacts during drought events (see table 1). P_{ALERT} is the average percentage of ALERT during the drought duration, and M_{ALERT} is the maximum percentage in the same period. The drought duration is defined as the period when the percentage of the NUTS with WATCH+WARNING+ALERT is > 20% for either CDI-v1 or CDI-v2.

NUTS	Period	duration (month)	CDI-v1		CDI-v2	
			P_{ALERT}	M_{ALERT}	P_{ALERT}	M_{ALERT}
DE1	1/2003 – 12/2003	9	12.4	70.4	25.9	79.5
ES42	7/2004 – 6/2006	16	18.9	73.6	42.8	88.5
RO31	1/2007 – 12/2007	5	20.3	44.9	41.2	71.4
RO12	9/2011 – 12/2012	13	5.9	36.9	17.3	45.5
ES62	1/2014 – 12/2014	10	10.2	78.2	31.8	83.0
SE21	1/2018 – 12/2018	5	4.3	10.8	8.1	18.8

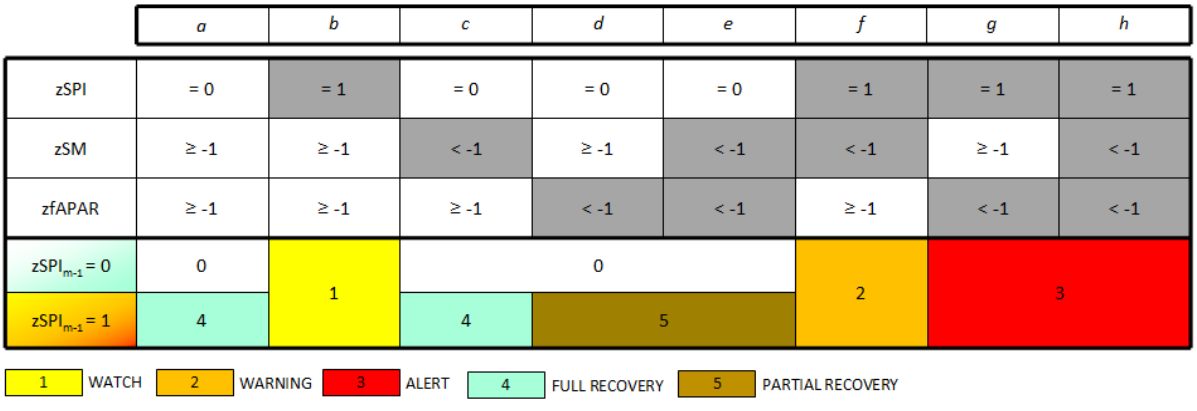

644

645 **Figure 1.** Schematic representation of the CDI-v1 computation procedure. The upper part of the
646 table reports the eight possible combinations of the three main Boolean quantities (from *a* to *h*).
647 The lower part of the table reports the corresponding CDI classes for the two possible cases of
648 antecedent zSPI (subscript m-1).

649

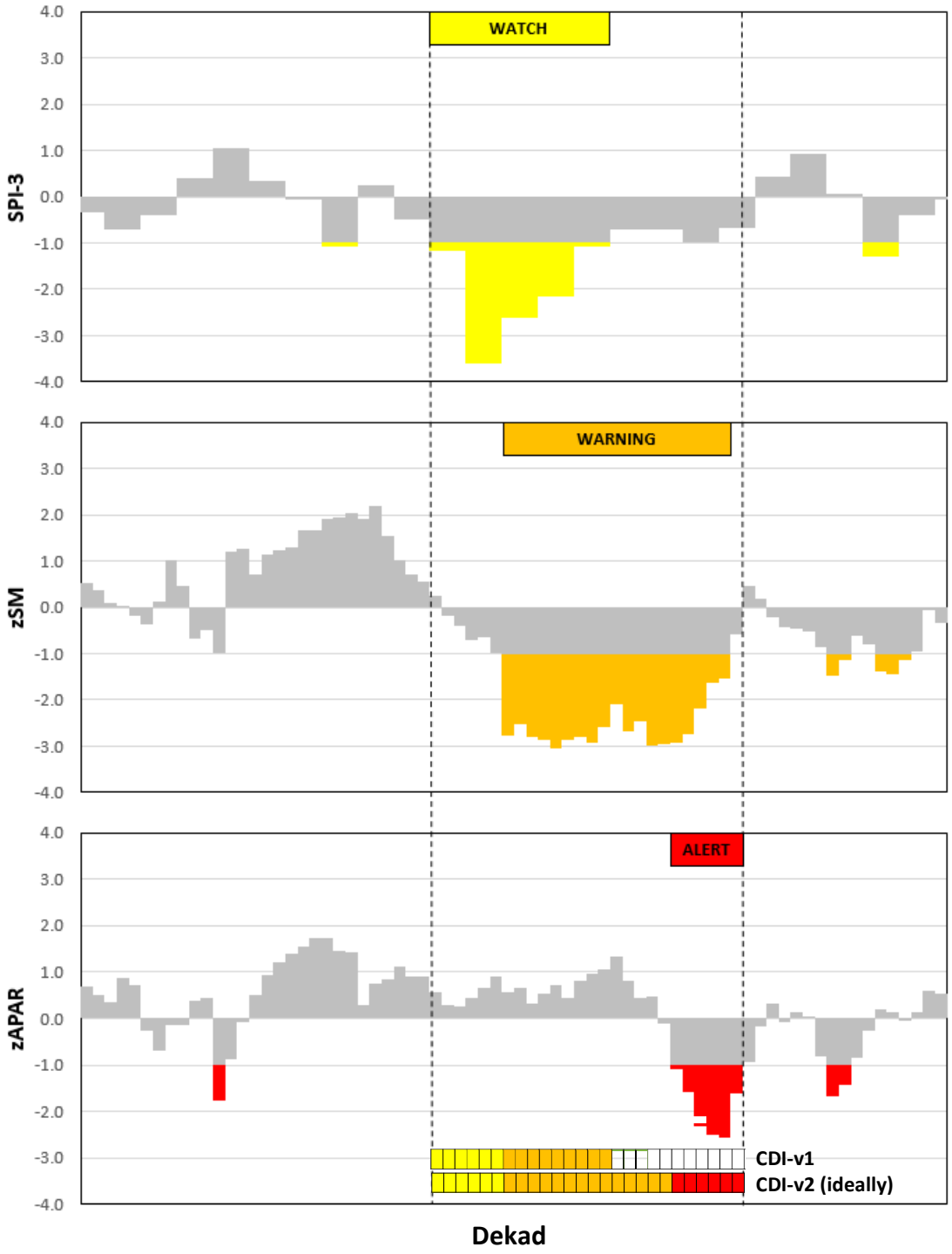

650

651 **Figure 2.** Example of the possible cascade process driving the evolution in a case of a drought
652 event in Spain. Dotted lines delimit the period under drought, whereas the squares at the bottom
653 of the plots report the outcome of the operational CDI (CDI-v1, upper line) and the ideal evolution
654 of a revised version (CDI-v2 ideally, lower line) values for each dekad.

655

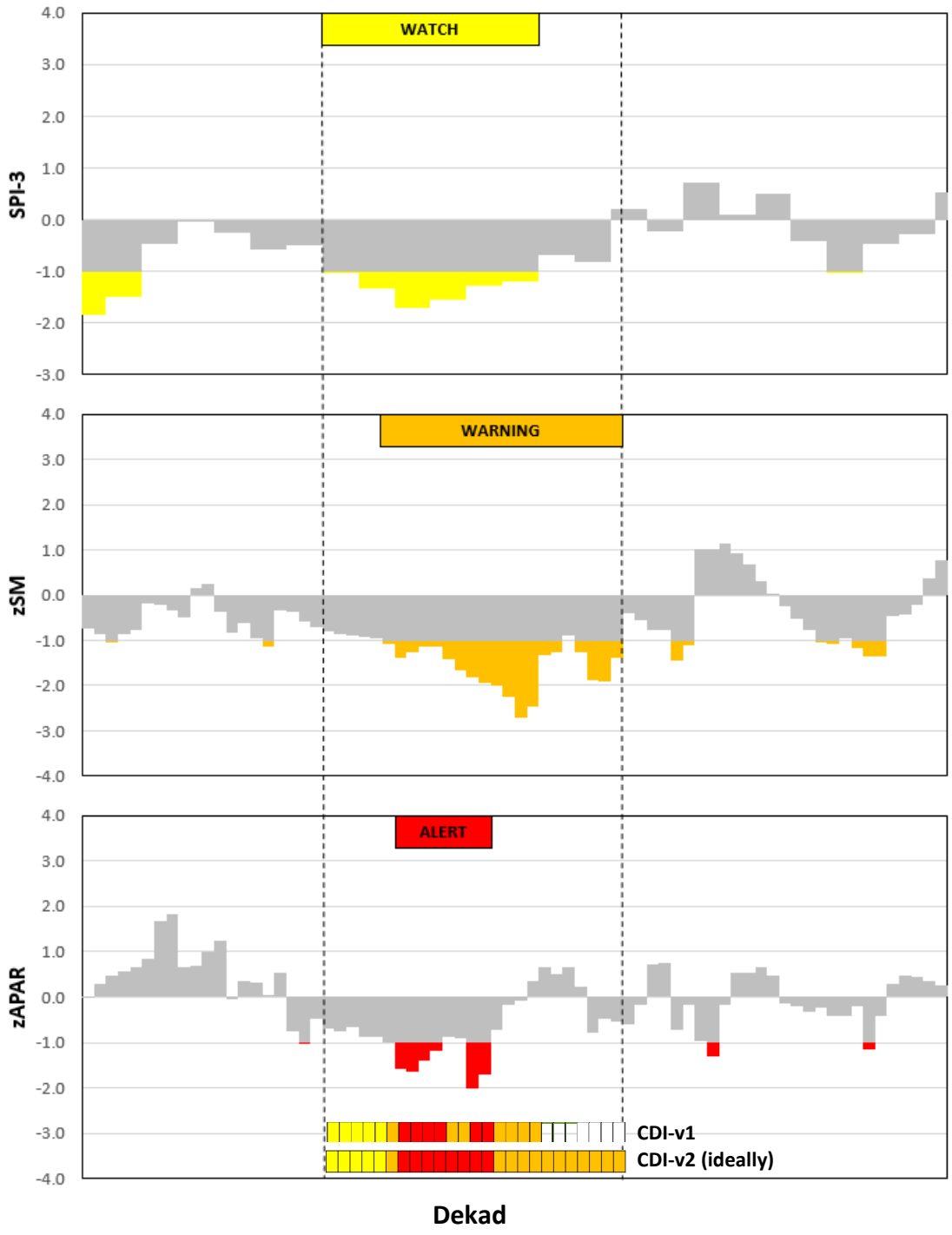

656

657 **Figure 3.** Example of the small gaps that can occur during a drought event in France. Dotted lines
658 delimit the period under drought, whereas the squares at the bottom of the plots report the
659 outcome of the operational CDI (CDI-v1, upper line) and the ideal evolution of a revised version
660 (CDI-v2 ideally, lower line) values for each dekad.

661

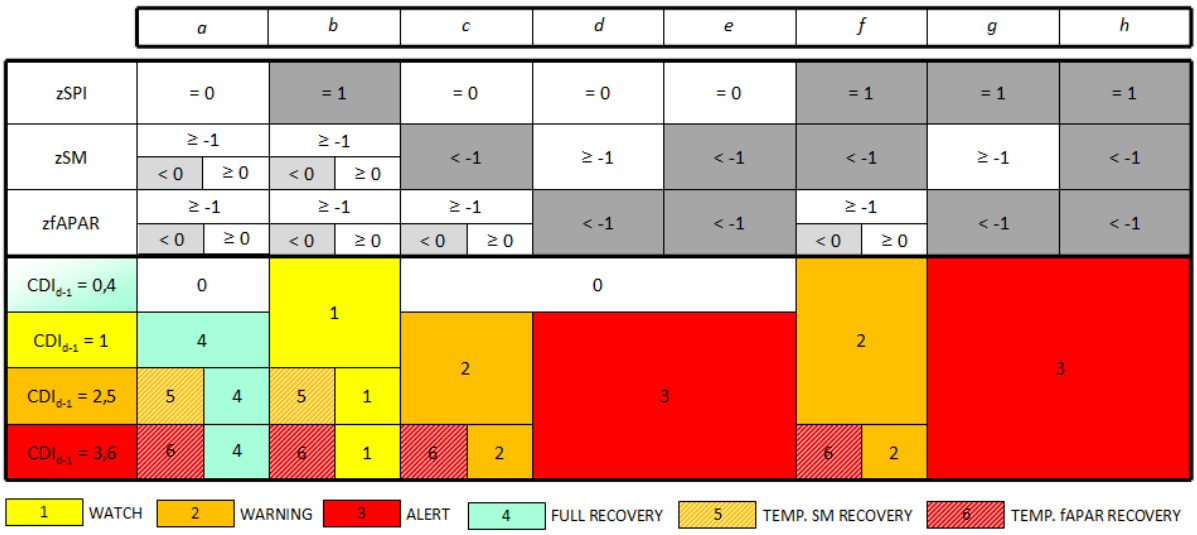

Figure 4. Schematic representation of the CDI-v2 computation procedure. The upper part of the table reports the eight possible combinations of the three main Boolean quantities (from *a* to *h*), with sub-cases (based on the second set of thresholds) reported where used. The lower part of the table reports the corresponding CDI classes for all the antecedent CDI values (subscript d-1).

667

668 **Figure 5.** Time series of CDI-v1 (upper lines) and CDI-v2 (lower lines) for different test sites under
669 drought between 2001 and 2011, as documented in Sepulcre-Canto et al. (2012). See Figs. 1 and 4
670 for the corresponding legends. The labels in the x-axis correspond to the beginning of the month.

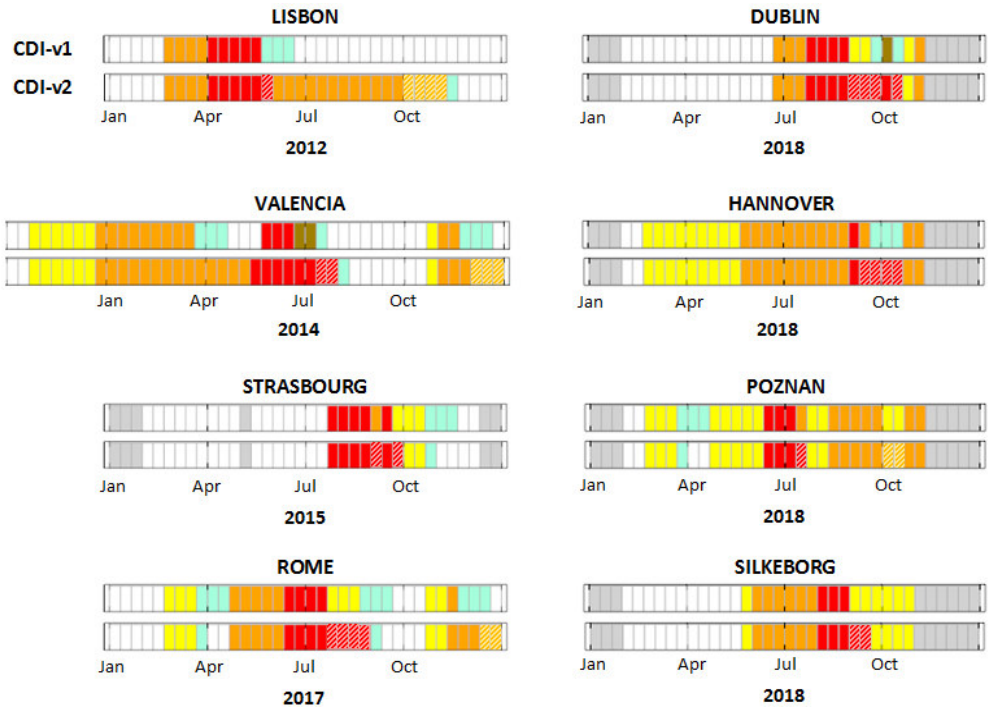

671

672 **Figure 6.** Time series of CDI-v1 (upper lines) and CDI-v2 (lower lines) for different test sites under
673 drought between 2012 and 2018, as documented in the analytical drought reports in EDO
674 (https://edo.jrc.ec.europa.eu/edov2/php/index.php?id=1051). See Figs. 1 and 4 for the
675 corresponding legends. The labels in the x-axis correspond to the beginning of the month.

676

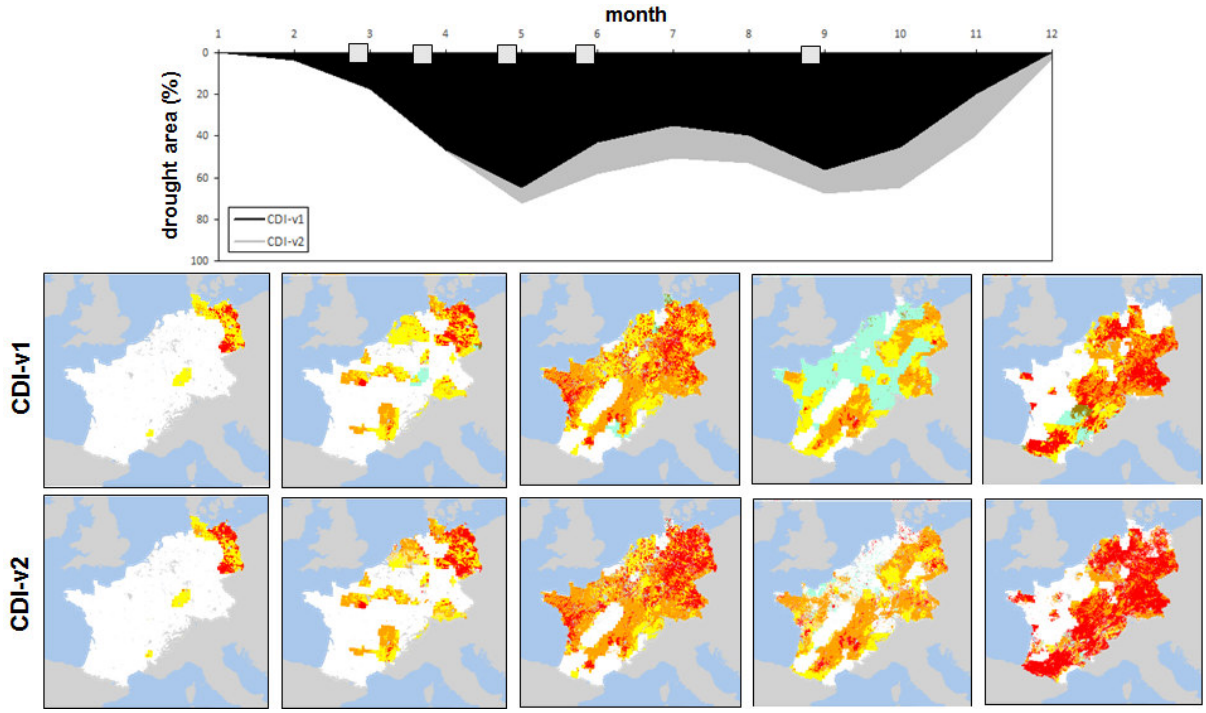

677

678 **Figure 7.** Temporal evolution of the 2003 central Europe drought according to the two versions of
679 the CDI. The upper plot shows the percentage of the area under drought
680 (WATCH+WARNING+ALERT, in black for CDI-v1 and in grey for CDI-v2), whereas the lower images
681 depict the spatial distribution of the CDI-v1 (upper row) and CDI-v2 (lower row) for the selected
682 dekads (demarked in the upper plot by the squares on the x-axis).

683

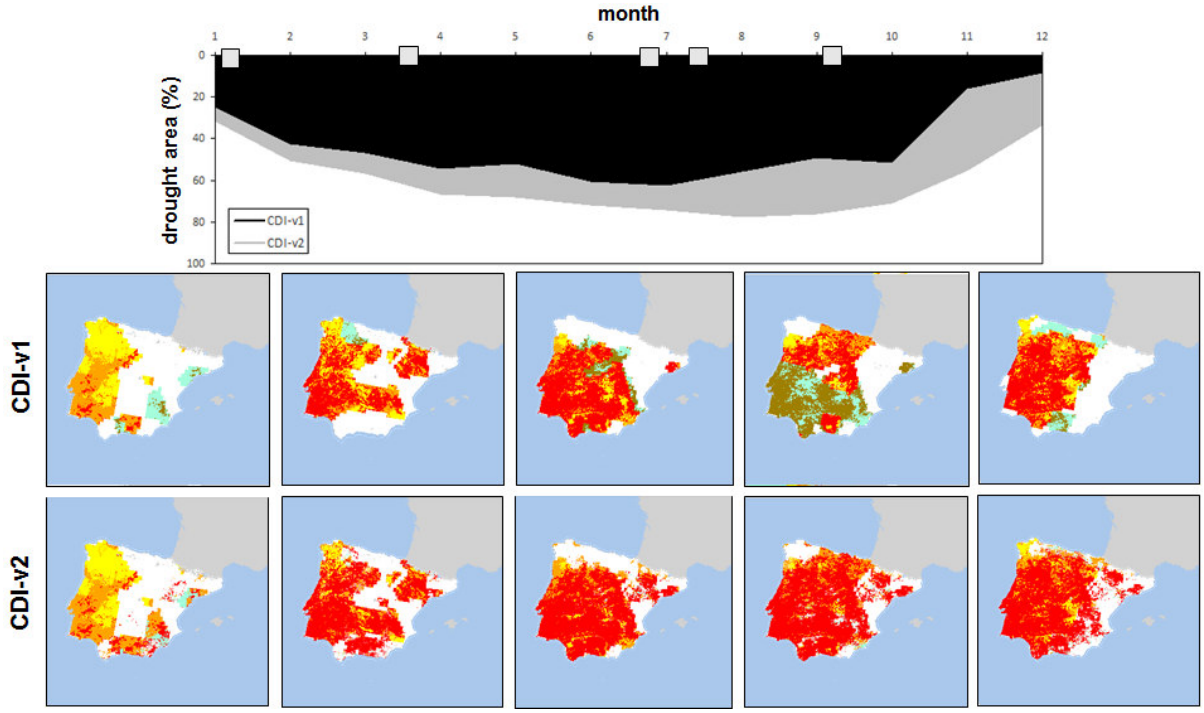

684

685 **Figure 8.** Temporal evolution of the 2005 Iberian Peninsula drought according to the two versions
686 of the CDI. The upper plot shows the percentage of the area under drought
687 (WATCH+WARNING+ALERT, in black for CDI-v1 and in grey for CDI-v2), whereas the lower images
688 depict the spatial distribution of the CDI-v1 (upper row) and CDI-v2 (lower row) for the selected
689 dekads (demarked in the upper plot by the squares on the x-axis).

690

691

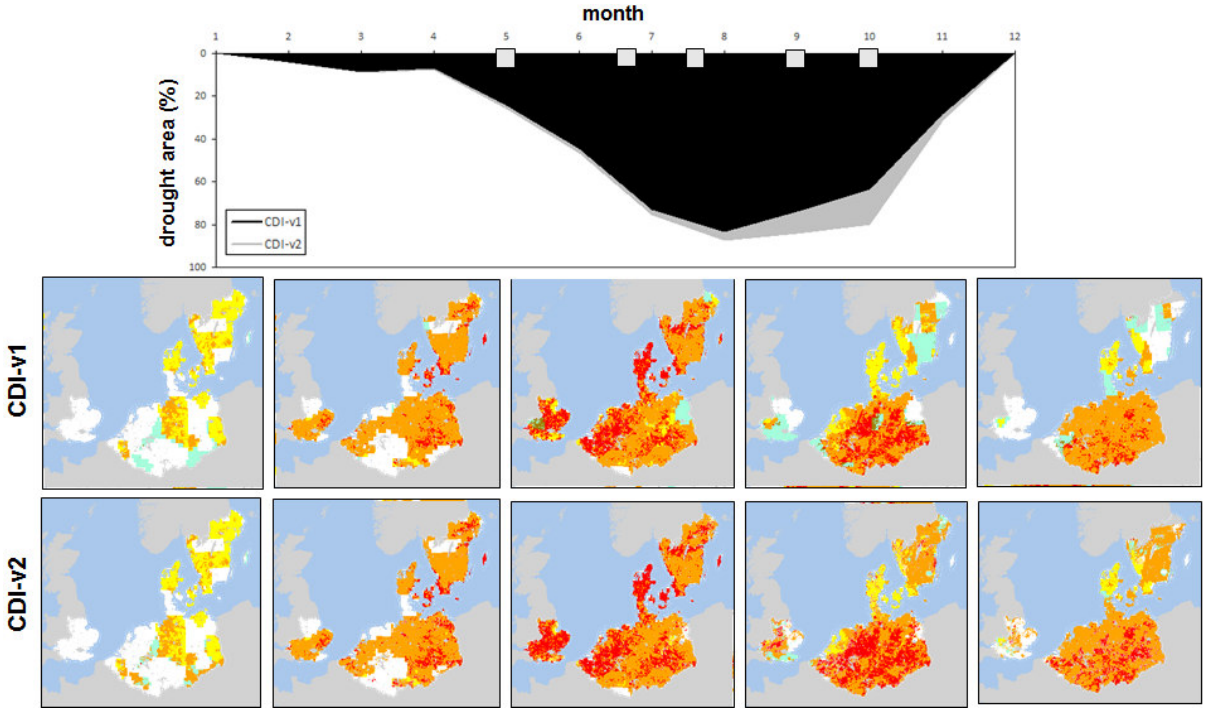

692

693 **Figure 9.** Temporal evolution of the 2018 northern Europe drought according to the two versions
694 of the CDI. The upper plot shows the percentage of the area under drought
695 (WATCH+WARNING+ALERT, in black for CDI-v1 and in grey for CDI-v2), whereas the lower images
696 depict the spatial distribution of the CDI-v1 (upper row) and CDI-v2 (lower row) for the selected
697 dekads (demarked in the upper plot by the squares on the x-axis).

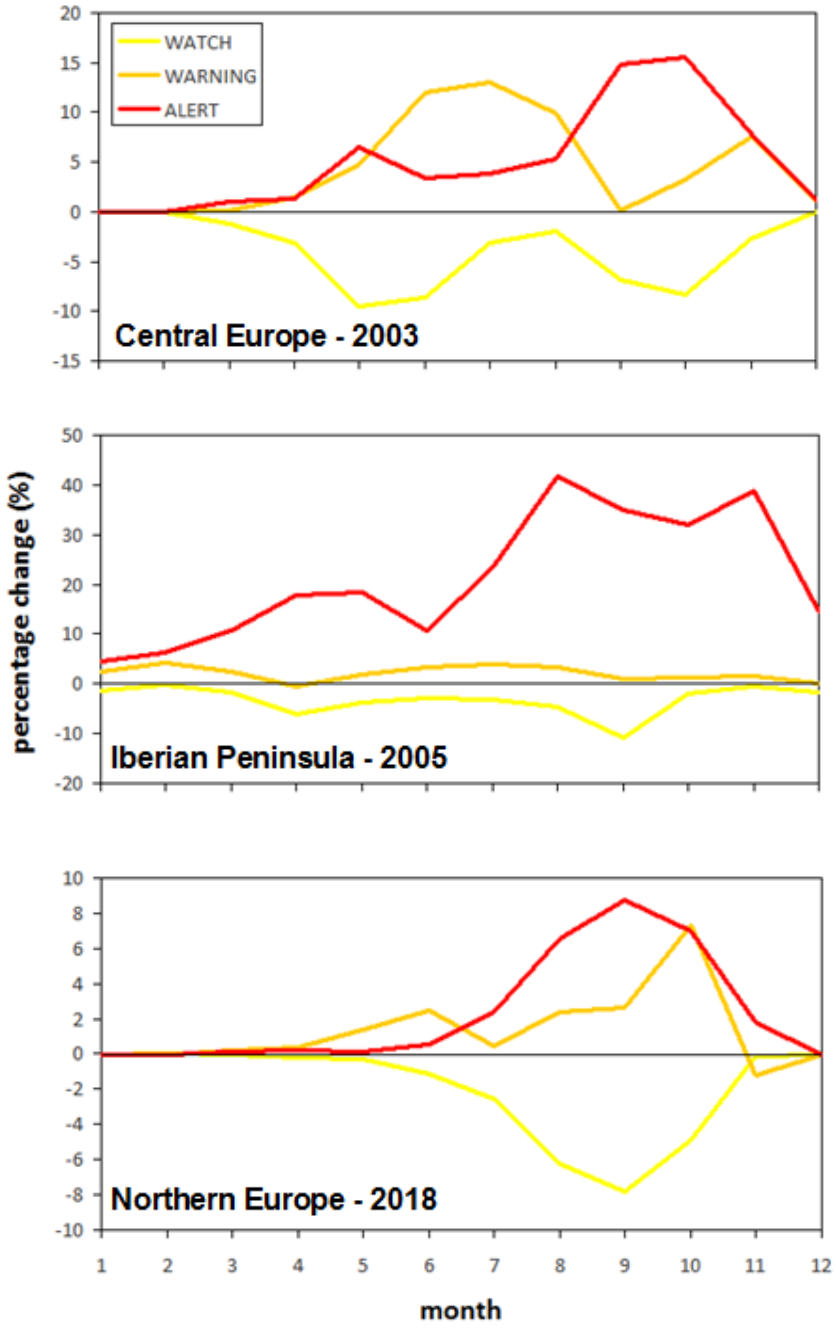

Figure 10. Percentage differences between CDI-v1 and CDI-v2 fraction of area in WATCH (yellow line), WARNING (orange line) and ALERT (red line) stages for the same three main droughts depicted in Figs. 7-9. Negative (positive) values indicate a reduction (increase) in the CDI-v2 compared to CDI-v1.